

Molecular and spectroscopic properties of chloride and thiocyanate hydridecarbonyl ruthenium(II) complexes with pyridine derivative ligands

J.G. Małecki*, A. Maroń

Department of Crystallography, Institute of Chemistry, University of Silesia, 9th Szkolna St., 40-006 Katowice, Poland

ARTICLE INFO

Article history:

Received 26 December 2010

Accepted 28 January 2011

Available online 7 March 2011

Keywords:

Ruthenium hydrido-carbonyl complexes

Ruthenium thiocyanate complexes

2,2'-Dipyridylamine

4-(3-Phenylpropyl)pyridine

X-ray structure

UV-Vis

Luminescence

DFT

TD-DFT

ABSTRACT

[RuH(CO)(dpa)(PPh₃)₂]X and [RuHX(CO)(pyCHPh)(PPh₃)₂] (X = Cl, NCS) complexes (where dpa = 2,2'-dipyridylamine, pyCHPh = 4-(3-phenylpropyl)pyridine) have been prepared and studied using IR, NMR, UV-Vis spectroscopies and X-ray crystallography. The electronic structures and bonding of the obtained complexes were defined on the basis of the DFT method. The electronic spectra of the complexes were calculated and associated with the structure of the molecular orbitals of the complexes. The luminescence properties of the complexes were determined.

© 2011 Elsevier Ltd. All rights reserved.

1. Introduction

Pyridine type ligands have energetically low lying π -antibonding orbitals, which can accept electrons from filled d orbitals of metal atoms. As a consequence, they can exhibit charge transfer bands with interesting spectroscopic properties in the visible region [1]. Ligands containing a pyridine ring are wide studied and their π -donor properties are interesting. Their combination with other donor atoms should in principle afford complexes with tunable spectroscopic properties [2]. The hydride ligand, a powerful σ -donor, is found to be very efficient at compensating for electron deficiency at the metal central ion in complexes. The “trans effect” of the H⁻ ligand and the interaction between CO and N-donor ligands in *trans* positions to one another are stabilizing factors which explain the stability of these complexes [3]. They are interesting because of their properties. Additionally, luminescent metal complexes are a fascinating class of molecules that have found applications in many areas. Luminescent ruthenium(II) complexes, especially with bipyridyl type ligands, have been extensively studied [4–7]. Furthermore, phosphine hydride carbonyl ruthenium(II) complexes with N-donor ligands are still of interest for their potential applications [8–12]. Hence, the synthesis and spectral characterization of new ruthenium complexes containing triphenylphosphine are of great importance.

Here, we present the synthesis, crystal, molecular and electronic structures, and spectroscopy characterization of two pairs of hydrido-carbonyl complexes of ruthenium(II) with 2,2'-dipyridylamine (dpa) (**1**), and 4-(3-phenylpropyl)pyridine (pyCHPh) (**2**) ligands. The complexes are synthesized as the chloride and thiocyanate derivatives. The luminescent properties of the complexes were examined. The experimental studies on the thiocyanate and chloride complexes have been accompanied computationally by density functional theory (DFT) calculations. Currently, DFT is commonly used to examine the electronic structure of transition metal complexes. It meets with the requirements of being accurate, easy to use and fast enough to render studies of relatively large molecules of transition metal complexes possible. DFT and TDDFT calculations were performed to establish the nature of the orbitals involved in the transition processes and to correlate the structural parameters with the spectroscopic properties of the complexes. It is known that thiocyanate ligands tune the t_{2g} ruthenium orbital by distributing $4d_{Ru}$ energy levels over a wide energy range due to mixing with orbitals centered on the NCS ligand ($2p_N$, $2p_C$ and $3p_S$) [13]. The calculated density of states showed that intermolecular as well as intramolecular interactions are important and significantly influence the orbital composition in the frontier electronic structure. Thus, studies of the electronic structures of complexes are an important area of chemistry. The complexes reported in this paper combine our interest in ruthenium coordination compounds and complexes containing pyridine derivatives ligands [14–17].

* Corresponding author.

E-mail address: gmalecki@us.edu.pl (J.G. Małecki).

2. Experimental

All reagents used for the synthesis of the complexes are commercially available and have been used without further purification. The $[\text{RuHCl}(\text{CO})(\text{PPh}_3)_3]$ complex was synthesized according to the literature method [18].

2.1. The synthesis of $[\text{RuH}(\text{CO})(\text{dpa})(\text{PPh}_3)_2]\text{Cl}\cdot\text{dpa}\cdot\text{CH}_3\text{OH}$ (**1**), $[\text{RuH}(\text{CO})(\text{dpa})(\text{PPh}_3)_2]\text{SCN}\cdot\text{H}_2\text{O}\cdot\text{CH}_3\text{OH}$ (**1a**) and $[\text{RuHCl}(\text{CO})(\text{pyCHPh})(\text{PPh}_3)_2]$ (**2**), $[\text{RuH}(\text{SCN})(\text{CO})(\text{pyCHPh})(\text{PPh}_3)_2]$ (**2a**)

The complexes were synthesized in the reaction between $[\text{RuHCl}(\text{CO})(\text{PPh}_3)_3]$ (1×10^{-4} mol) and 2,2'-dipyridylamine (dpa) (**1**), 4-(3-phenylpropyl)pyridine (pyCHPh) (**2**) (1.2×10^{-4} mol) and NH_4SCN (**1a** and **2a**) in methanol solutions (50 cm^{-3}). The mixture of reagents was refluxed in methanol for 3 h. After this time, it was cooled and filtered. Crystals suitable for X-ray crystal analysis were obtained by slow evaporation of the reaction mixture.

1: Yield 50%. IR (KBr, cm^{-1}): 3400 $\nu_{\text{NH/OH}}$; 3060, 3014 $\nu_{\text{ArH/CH}}$; 1994 $\nu_{(\text{Ru-H})}$; 1922 $\nu_{(\text{CO})}$; 1639 $\nu_{(\text{C=N})}$; 1590 $\nu_{(\text{C=N})}$ free dpa; 1520 $\nu_{(\text{C=C})}$ free dpa; 1476, 1310 $\delta_{(\text{C-CH in the plane})}$; 1434 $\nu_{\text{Ph(P-Ph)}}$; 1091 $\delta_{(\text{C-CH in the plane})}$; 774 $\delta_{(\text{C-C out of the plane})}$; 696 $\delta_{(\text{C-C in the plane})}$; 511 $\nu_{(\text{P-Ph} + \text{P-Ru})}$. UV–Vis (methanol, nm) (log ϵ): 360.5 (1.23), 310.4 (1.90), 260.1 (2.86), 213.3 (5.12). ^1H NMR (δ , CDCl_3): 11.392 (s, NH), 8.281–6.868 (m, dpa/ PPh_3), 3.501 (CH_3OH), –12.231 (t, H_{Ru} , $J = 19.19$ Hz). ^{31}P NMR (δ , CDCl_3): 48.424 (s, PPh_3).

1a: Yield 50%. IR (KBr, cm^{-1}): 3410 $\nu_{\text{NH/OH}}$; 2918 ν_{ArH} ; 2057 ν_{SCN} ; 1971 $\nu_{(\text{Ru-H})}$; 1923 $\nu_{(\text{CO})}$; 1641 $\nu_{(\text{C=N})}$; 1580 $\nu_{(\text{C=C})}$; 1477 $\delta_{(\text{C-CH in the plane})}$; 1432 $\nu_{\text{Ph(P-Ph)}}$; 1090 $\delta_{(\text{C-CH in the plane})}$; 816 $\delta_{(\text{SC})}$; 772 $\delta_{(\text{C-C out of the plane})}$; 695 $\delta_{(\text{C-C in the plane})}$; 517 $\delta_{(\text{NCS})}$. UV–Vis (methanol, nm) (log ϵ): 362.0 (1.31), 327.0 (1.79), 308.0 (2.10), 255.5 (4.66), 211.5 (5.02). ^1H NMR (δ , CDCl_3): 10.305 (s, NH), 7.804–6.194 (m, dpa/ PPh_3), 3.501 (CH_3OH), 1.613 (H_2O), –12.217 (t, H_{Ru} , $J = 19.69$ Hz). ^{31}P NMR (δ , CDCl_3): 47.996 (s, PPh_3).

Table 1

Crystal data and structure refinement details of the complexes $[\text{RuH}(\text{CO})(\text{dpa})(\text{PPh}_3)_2]\text{Cl}\cdot\text{dpa}\cdot\text{CH}_3\text{OH}$ (**1**), $[\text{RuH}(\text{CO})(\text{dpa})(\text{PPh}_3)_2]\text{SCN}\cdot\text{H}_2\text{O}\cdot\text{CH}_3\text{OH}$ (**1a**), $[\text{RuHCl}(\text{CO})(\text{pyCHPh})(\text{PPh}_3)_2]$ (**2**) and $[\text{RuH}(\text{SCN})(\text{CO})(\text{pyCHPh})(\text{PPh}_3)_2]$ (**2a**).

	1	1a	2	2a
Empirical formula	$\text{C}_{58}\text{H}_{53}\text{ClN}_6\text{O}_2\text{P}_2\text{Ru}$	$\text{C}_{49}\text{H}_{46}\text{N}_4\text{O}_3\text{P}_2\text{RuS}$	$\text{C}_{51}\text{H}_{46}\text{ClN}_6\text{O}_2\text{Ru}$	$\text{C}_{52}\text{H}_{46}\text{N}_2\text{OP}_2\text{RuS}$
Formula weight	1064.52	933.97	887.35	909.98
<i>T</i> (K)	295(2)	295(2)	295(2)	295(2)
Crystal system	triclinic	monoclinic	triclinic	monoclinic
Space group	$P\bar{1}$	$P2_1/c$	$P\bar{1}$	$P2_1/n$
<i>Unit cell dimensions</i>				
<i>a</i> (Å)	13.679(3)	9.866(3)	13.009(3)	13.269(9)
<i>b</i> (Å)	14.347(4)	14.252(4)	13.276(4)	14.930(10)
<i>c</i> (Å)	15.156(5)	31.797(10)	13.276(3)	23.967(13)
α (°)	98.077(3)	90	76.064(2)	90
β (°)	116.474(4)	97.230(3)	75.894(2)	100.736(6)
γ (°)	97.915(3)	90	87.776(19)	90
<i>V</i> [Å ³]	2567.75(16)	4435.3(2)	2157.71(9)	4664.7(5)
<i>Z</i>	2	4	2	4
<i>D</i> _{calc} (Mg/m ³)	1.377	1.399	1.366	1.296
Absorption coefficient (mm ⁻¹)	0.469	0.519	0.538	0.488
<i>F</i> (0 0 0)	1100	1928	916	1880
Crystal dimensions (mm)	0.18 × 0.15 × 0.05	0.32 × 0.18 × 0.09	0.38 × 0.27 × 0.10	0.35 × 0.26 × 0.19
θ range for data collection (°)	3.36 to 25.05	3.45 to 25.05	3.47 to 25.05	3.37 to 25.05
Index ranges	–16 ≤ <i>h</i> ≤ 16 –17 ≤ <i>k</i> ≤ 16 –13 ≤ <i>l</i> ≤ 18	–11 ≤ <i>h</i> ≤ 11 –16 ≤ <i>k</i> ≤ 16 –30 ≤ <i>l</i> ≤ 37	–15 ≤ <i>h</i> ≤ 15 –15 ≤ <i>k</i> ≤ 15 –15 ≤ <i>l</i> ≤ 15	–12 ≤ <i>h</i> ≤ 15 –17 ≤ <i>k</i> ≤ 12 –28 ≤ <i>l</i> ≤ 28
Reflections collected	18 677	29 457	39 769	15 767
Independent reflections (<i>R</i> _{int})	9008 (0.0295)	7804 (0.0349)	7632 (0.0316)	8232 (0.0355)
Data/restraints/parameters	9008/0/636	7804/0/555	7632/0/518	8232/0/536
Goodness-of-fit on <i>F</i> ²	0.939	1.177	1.058	1.038
Final <i>R</i> indices [<i>I</i> > 2σ(<i>I</i>)]	<i>R</i> ₁ = 0.0309 <i>wR</i> ₂ = 0.0688	<i>R</i> ₁ = 0.0468 <i>wR</i> ₂ = 0.0921	<i>R</i> ₁ = 0.0275 <i>wR</i> ₂ = 0.0719	<i>R</i> ₁ = 0.0363 <i>wR</i> ₂ = 0.0762
<i>R</i> indices (all data)	<i>R</i> ₁ = 0.0475 <i>wR</i> ₂ = 0.0713	<i>R</i> ₁ = 0.0560 <i>wR</i> ₂ = 0.0943	<i>R</i> ₁ = 0.0392 <i>wR</i> ₂ = 0.0753	<i>R</i> ₁ = 0.0531 <i>wR</i> ₂ = 0.1187
Largest difference in peak and hole (e Å ⁻³)	0.571 and –0.606	0.460 and –0.624	0.396 and –0.257	1.192 and –1.450

2: Yield 62%. IR (KBr, cm^{-1}): 3052 ν_{ArH} ; 2928, 2854 ν_{CH} ; 2000 $\nu_{(\text{Ru-H})}$; 1925 $\nu_{(\text{CO})}$; 1642 $\nu_{(\text{C=N})}$; 1616 $\nu_{(\text{C=C})}$; 1479 $\delta_{(\text{C-CH in the plane})}$; 1432 $\nu_{\text{Ph(P-Ph)}}$; 1092 $\delta_{(\text{C-CH in the plane})}$; 746 $\delta_{(\text{C-C out of the plane})}$; 694 $\delta_{(\text{C-C in the plane})}$; 510 $\nu_{(\text{P-Ph} + \text{P-Ru})}$. UV–Vis (methanol, nm) (log ϵ): 332.0 (1.46), 256.2 (2.56), 210.6 (5.02). ^1H NMR (δ , CDCl_3): 8.262 (d, H₂/6_{py}), 7.604–7.222 (m, Ph/ PPh_3), 6.495 (s, H₃/5_{py}), 2.586, (CH_2), 2.193 (CH_2), 1.113 (CH_2), –13.517 (t, H_{Ru} , $J = 19.69$ Hz). ^{31}P NMR (δ , CDCl_3): 45.666 (s, PPh_3), 43.247 (s, PPh_3).

2a: Yield 65%. IR (KBr, cm^{-1}): 3051 ν_{ArH} ; 2938, 2856 ν_{CH} ; 2091 ν_{SCN} ; 2001 $\nu_{(\text{Ru-H})}$; 1934 $\nu_{(\text{CO})}$; 1617 $\nu_{(\text{C=N})}$; 1586 $\nu_{(\text{C=C})}$; 1480 $\delta_{(\text{C-CH in the plane})}$; 1433 $\nu_{\text{Ph(P-Ph)}}$; 1093 $\delta_{(\text{C-CH in the plane})}$; 797 $\delta_{(\text{SC})}$; 746 $\delta_{(\text{C-C out of the plane})}$; 694 $\delta_{(\text{C-C in the plane})}$; 519 $\delta_{(\text{SC})}$; 512 $\nu_{(\text{P-Ph} + \text{P-Ru})}$. UV–Vis (methanol, nm) (log ϵ): 328.4 (1.19), 276.2 (1.37), 252.1 (2.96), 211.0 (4.98). ^1H NMR (δ , CDCl_3): 8.523 (d, H₂/6_{py}), 7.542–7.186 (m, Ph/ PPh_3), 6.506 (s, H₃/5_{py}), 2.611, 2.450, 2.326 (CH_2), 1.846, 1.761 (CH_2), 1.580, 1.284 (CH_2), –12.619 (td, H_{Ru} , $J = 19.35$ Hz). ^{31}P NMR (δ , CDCl_3): 46.794 (s, PPh_3), 44.874 (s, PPh_3).

2.2. Physical measurements

Infrared spectra were recorded on a Perkin–Elmer spectrophotometer in the spectral range 4000–450 cm^{-1} using KBr pellets. Electronic spectra were measured on a Lab Alliance UV–VIS 8500 spectrophotometer in the range 500–180 nm in methanol solution. ^1H and ^{31}P NMR spectra were obtained at room temperature in CDCl_3 using a Bruker 400 spectrometer. Luminescence measurements were made in methanolic solutions on an F-2500 FL spectrophotometer at room temperature.

2.3. DFT calculations

The calculations were carried out using the GAUSSIAN09 [19] program. The DFT/B3LYP/CAM-B3LYP [20,21] method was used for the geometry optimization and electronic structure determination, and electronic spectra were calculated by the TD-DFT [22] method.

The calculations were performed using a DZVP basis set [23] with f functions having exponents of 1.94722036 and 0.748930908 for the ruthenium atom, and polarization functions for all other atoms: 6-31g** – sulfur, carbon, nitrogen and 6-31g – hydrogen. The PCM (Polarizable Continuum Model) solvent model was used in the Gaussian calculations, with methanol as the solvent. Natural bond orbital (NBO) calculations were performed with the NBO code [24] included in GAUSSIAN09. The contribution of a group to a molecular orbital was calculated using Mulliken population analysis. GAUSSSUM 2.2 [25] was used to calculate group contributions to molecular orbitals and to prepare partial density of states (DOS) spectra. The DOS spectra were created by convoluting the molecular orbital information with Gaussian curves of unit height and a FWHM (Full Width at Half Maximum) of 0.3 eV. Mayer bond orders were calculated with use of the QMFORGE program [26].

2.4. Crystal structure determinations and refinements

Pale yellow plate crystals of $[\text{RuH}(\text{CO})(\text{dpa})(\text{PPh}_3)_2]\text{Cl-dpa}^-$ CH_3OH (**1**), $[\text{RuH}(\text{CO})(\text{dpa})(\text{PPh}_3)_2]\text{SCN}\cdot\text{H}_2\text{O}\cdot\text{CH}_3\text{OH}$ (**1a**), $[\text{RuHCl}(\text{CO})(\text{pyCHPh})(\text{PPh}_3)_2]$ (**2**) and $[\text{RuH}(\text{SCN})(\text{CO})(\text{pyCHPh})(\text{PPh}_3)_2]$ (**2a**) were mounted in turn on an Xcalibur, Atlas, Gemini Ultra Oxford Diffraction automatic diffractometer equipped with a CCD detector, and were used for data collection. X-ray intensity data were collected with graphite monochromated Mo $K\alpha$ radiation ($\lambda = 0.71073 \text{ \AA}$) at a temperature of 295(2) K, with the ω scan mode. Ewald sphere reflections were collected up to $2\theta = 50.10^\circ$. The unit cell parameters were determined from least-squares refinement of the setting angles of 11 167, 16 717, 23 955 and 6472 strongest reflections for complexes **1**, **1a**, **2** and **2a** respectively. Details concerning crystal data and refinement are gathered

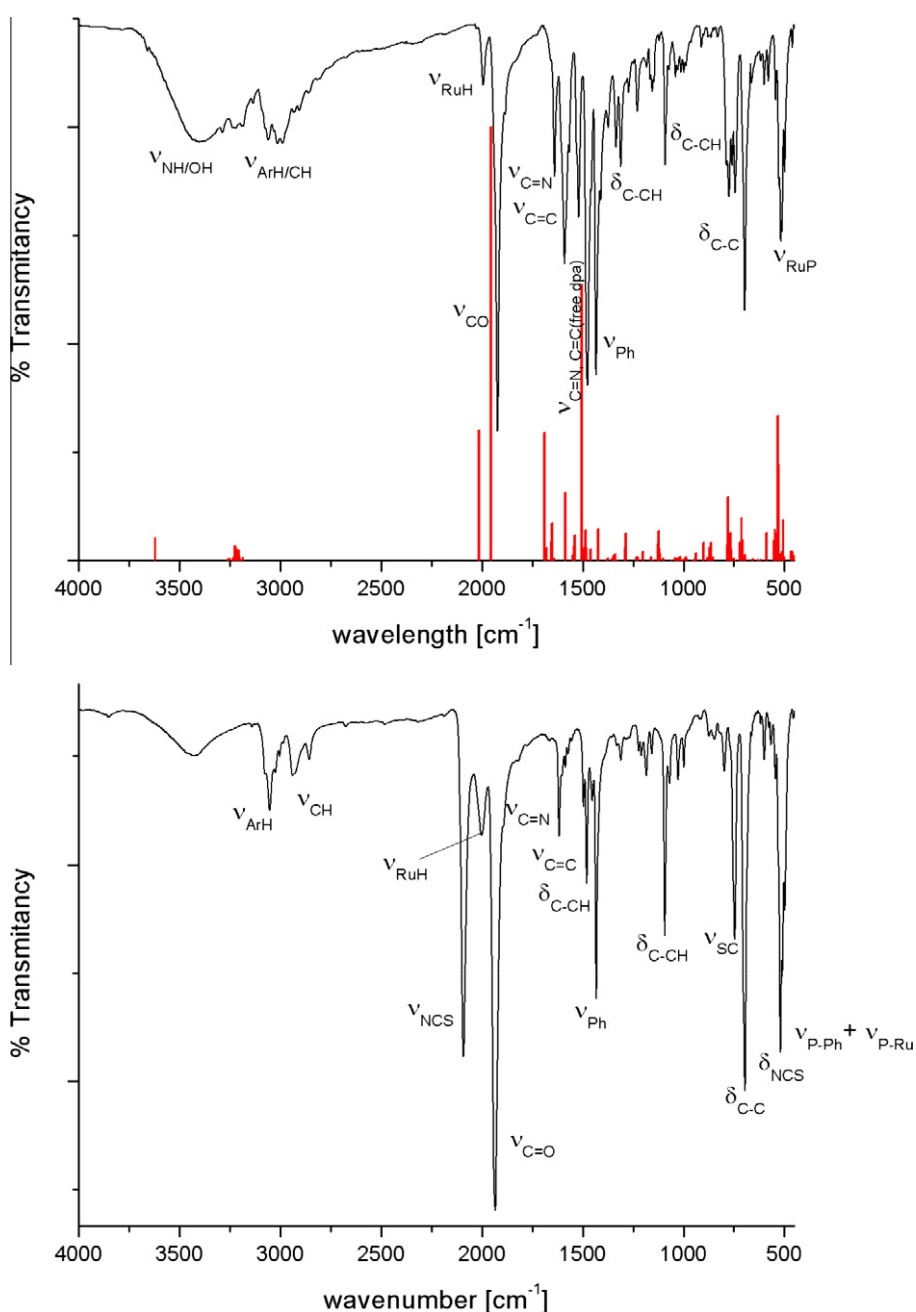


Fig. 1. IR spectra of the complexes $[\text{RuH}(\text{CO})(\text{dpa})(\text{PPh}_3)_2]\text{Cl-dpa}^- \text{CH}_3\text{OH}$ (**1**) and $[\text{RuH}(\text{SCN})(\text{CO})(\text{pyCHPh})(\text{PPh}_3)_2]$ (**2a**).

in Table 1. During the data reduction, the decay correction coefficient was taken into account. Lorentz, polarization and numerical absorption corrections were applied. The structures were solved by the Patterson method. All the non-hydrogen atoms were refined anisotropically using the full-matrix, least-squares technique on F^2 . The Ru–H hydrogen atoms were found from difference Fourier synthesis after four cycles of anisotropic refinement, and refined as “riding” on the adjacent atom with an individual isotropic temperature factor equal to 1.2 times the value of the equivalent temperature factor of the parent atom, with geometry idealization after each cycle. The OLEX2 [27] and SHELXS97, SHELXL97 [28] programs were used for all the calculations. Atomic scattering factors were those incorporated in the computer programs.

3. Results and discussion

$[\text{RuH}(\text{CO})(\text{dpa})(\text{PPh}_3)_2]\text{Cl}\cdot\text{dpa}\cdot\text{CH}_3\text{OH}$ (**1**) and $[\text{RuHCl}(\text{CO})(\text{pyCHPh})(\text{PPh}_3)_2]$ (**2**) complexes were obtained by the reaction of $[\text{RuHCl}(\text{CO})(\text{PPh}_3)_3]$ with 2,2'-dipyridylamine (dpa) and 4-(3-phenylpropyl)pyridine (pyCHPh) in methanol solutions. Isothiocyanate analogs $[\text{RuH}(\text{CO})(\text{dpa})(\text{PPh}_3)_2]\text{SCN}\cdot\text{H}_2\text{O}\cdot\text{CH}_3\text{OH}$ (**1a**) and

$[\text{RuH}(\text{SCN})(\text{CO})(\text{pyCHPh})(\text{PPh}_3)_2]$ (**2a**) were synthesized using NH_4SCN in the reactions. The ^1H NMR spectra of the complexes displayed sets of signals, given in the experimental section, that were ascribed to the N-heteroaromatic and triphenylphosphine ligands. The triplets at -12.231 , -12.217 , -13.517 and -12.619 ppm indicate a hydride ligand in the complexes **1**, **1a**, **2** and **2a** respectively. Singlets in the ^{31}P NMR spectra of complexes **1** and **1a** at 48.424 and 47.996 ppm indicate both triphenylphosphine ligands in the compounds are equivalent and they are mutually *trans* disposed. In the ^{31}P NMR spectra of complexes **2** and **2a**, two singlets at 45.666, 43.247 and 46.794, 44.874 ppm indicate that the PPh_3 ligands are not exactly *trans* disposed.

IR spectra of the complexes present ring C=N stretching modes of the pyridine derivative ligands at 1639 and 1642 cm^{-1} for the chloride complexes **1** and **2**, and at 1641 and 1617 cm^{-1} in the isothiocyanate derivatives **1a** and **2a**, respectively. In the spectrum of complex **1**, C=N and C=C stretches of a free ligand are observed at 1590 and 1520 cm^{-1} . NH and OH (methanol) groups are indicated by a broad band with a maximum at 3400 cm^{-1} . The intense bands with maxima near 2000 cm^{-1} in the IR spectra indicate the presence of hydride ligands in the complexes, and stretching modes

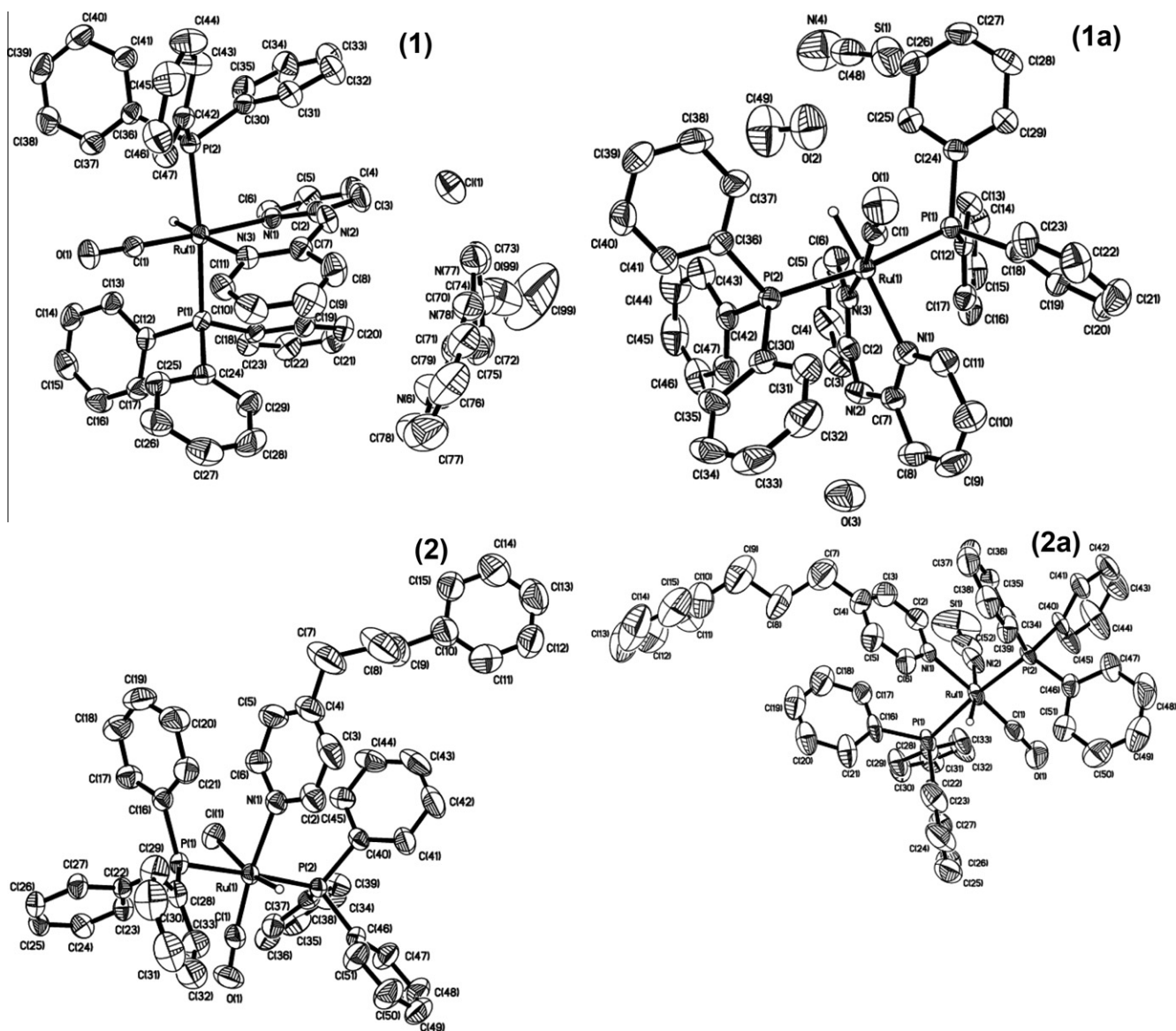


Fig. 2. ORTEP drawing of the complexes $[\text{RuH}(\text{CO})(\text{dpa})(\text{PPh}_3)_2]\text{Cl}\cdot\text{dpa}\cdot\text{CH}_3\text{OH}$ (**1**), $[\text{RuH}(\text{CO})(\text{dpa})(\text{PPh}_3)_2]\text{SCN}\cdot\text{H}_2\text{O}\cdot\text{CH}_3\text{OH}$ (**1a**), $[\text{RuHCl}(\text{CO})(\text{pyCHPh})(\text{PPh}_3)_2]$ (**2**) and $[\text{RuH}(\text{SCN})(\text{CO})(\text{pyCHPh})(\text{PPh}_3)_2]$ (**2a**) with 50% probability displacement ellipsoids. Hydrogen atoms (except for Ru–H) are omitted for clarity.

of the carbonyl group are observed at 1922, 1923, 1925 and 1934 cm^{-1} for complexes **1**, **1a**, **2** and **2a**, respectively. Three characteristic bands are observed at 2057, 816 and 517 cm^{-1} in the IR spectrum of **1a**, and at 2091, 797 and 519 cm^{-1} for **2a**, ascribed to ν_{CN} , ν_{CS} and δ_{NCS} respectively. Fig. 1 presents the IR spectra of complexes **1** and **2a**. For N-bonded complexes, generally the C–N stretching band is in a lower region, around 2050 cm^{-1} , compared to that of 2100 cm^{-1} for S-bonded complexes. However, the frequencies of the bands are sensitive to other factors like coexisting ligands, and the structure of the compounds were determined using X-ray analysis. While M–S–C angles of S-bonded thiocyanato ligands in complexes are bent, at around 110°, M–N–C angles of N-bonded isothiocyanato ligands are close to linear. The Ru(1)–N(2)–C(52) angle in complex **2a** is 169.2(8)°, indicating an isothiocyanato ligand. The *trans* effect of the H^- ligand results in an elongation of the Ru(1)–N(3) bond in complexes **1** and **1a** by about 0.05 Å compared to the Ru(1)–N(1) bond distances. The chloride complexes crystallize in the triclinic space group $P\bar{1}$ and the isothiocyanato analogs – in the monoclinic $P2_1/c$ and $P2_1/n$ space groups. The molecular structures of the complexes are shown in Fig. 2. Selected bond lengths and angles are listed in Table 2. In the complexes, the ruthenium atoms have a disordered octahedral environment. The triphenylphosphine ligands in complexes **2** and **2a** are not in perfect *trans* positions, which coincides with the ^{31}P NMR data. In the case of complex **1**, the solvent (methanol) molecule is better modeled as disordered, but the differences in *R* factors are very small (3.09 and 3.04 with disorder). A similar situation occurs in the case of a free dpa molecule (for atoms C76–

C78). The coordinated molecule of dpa shows also a sign of disorder, but it is rather dynamical in character.

3.1. Electronic structure

To obtain an insight into the electronic structures and bonding properties of the complexes, calculations using the density functional theory (DFT) method were carried out. Before the calculations, their geometries were optimized in singlet states using the DFT method with the B3LYP functional. In general, the predicted bond lengths and angles are in good agreement with the values based on the X-ray crystal structure data, and the general trends observed in the experimental data are well reproduced in the calculations (Table 2). As an example, the calculated IR frequencies of **1** are presented in Fig. 1.

The densities of states (DOS) in terms of Mulliken population analysis were calculated using the GAUSSSUM program, and Fig. 3 presents the composition of the fragment orbitals contributing to the molecular orbitals. As can be seen from Fig. 3, the d_{Ru} orbitals play a significant role in the frontier Homo orbitals of the complexes. The contributions of *d* orbitals of the ruthenium central ions in occupied molecular orbitals are in the range 45–60% (Homo–Homo – 3) in the cationic complex **1**, and 25–50% (Homo–Homo – 6) in complex **2**. In the thiocyanate analogs, the values vary from 30% to 48% in **1a** and 13% to 71% in neutral complex **2a**. In these molecular orbitals, the triphenylphosphine ligands play a significant role. As can be seen from the DOS diagrams, the 2,2'-dipyridylamine ligand contributes in a wider range of

Table 2

Selected bond lengths (Å) and angles (°) for the complexes $[\text{RuH}(\text{CO})(\text{dpa})(\text{PPh}_3)_2]\text{Cl}\cdot\text{dpa}\cdot\text{CH}_3\text{OH}$ (**1**), $[\text{RuH}(\text{CO})(\text{dpa})(\text{PPh}_3)_2]\text{SCN}\cdot\text{H}_2\text{O}\cdot\text{CH}_3\text{OH}$ (**1a**), $[\text{RuHCl}(\text{CO})(\text{pyCHPh})(\text{PPh}_3)_2]$ (**2**) and $[\text{RuH}(\text{SCN})(\text{CO})(\text{pyCHPh})(\text{PPh}_3)_2]$ (**2a**).

	1		1a	2		2a
	exp	calc		exp	calc	
<i>Bond lengths [Å]</i>						
Ru(1)–C(1)	1.828(2)	1.852	1.837(4)	1.823(3)	1.858	1.829(9)
Ru(1)–N(1)	2.150(18)	2.181	2.156(3)	2.203(19)	2.274	2.191(6)
Ru(1)–N(3)/N(2)	2.197(18)	2.252	2.219(3)			2.169(9)
Ru(1)–P(1)	2.384(6)	2.428	2.385(9)	2.362(5)	2.436	2.360(18)
Ru(1)–P(2)	2.369(6)	2.408	2.366(10)	2.352(5)	2.424	2.348(17)
Ru(1)–Cl(1)				2.537(6)	2.605	
Ru–H1(Ru)	1.55(2)	1.59	1.55(4)	1.56(2)	1.60	1.62(5)
C(1)–O(1)	1.157(3)	1.159	1.152(5)	1.154(3)	1.162	1.156(12)
N–C(S)			1.143(8)			1.110(11)
S–C(N)			1.599(7)			1.630(12)
<i>Angles (°)</i>						
P(1)–Ru(1)–P(2)	170.77(2)	169.22	172.55(3)	176.39(19)	175.66	169.64(8)
C(1)–Ru(1)–N(3)/N(2)	97.71(8)	99.93	172.83(14)			97.80(3)
P(1)–Ru(1)–N(1)	90.76(5)	91.38	92.06(8)	90.09(5)	89.61	92.33(14)
P(1)–Ru(1)–C(1)	89.18(7)	89.42	89.74(12)	90.57(7)	88.56	86.50(2)
N(1)–Ru(1)–N(3)/N(2)	88.14(7)	85.95	86.51(11)			87.20(3)
P(2)–Ru(1)–N(1)	89.50(5)	91.33	95.33(8)	91.34(5)	92.72	89.83(14)
P(2)–Ru(1)–C(1)	89.63(7)	86.83	89.76(12)	87.44(7)	88.59	90.40(2)
P(2)–Ru(1)–N(3)/N(2)	97.93(5)	97.63	89.02(8)			97.90(2)
P(1)–Ru(1)–N(3)/N(2)	91.29(5)	92.96	90.56(8)			92.30(2)
N(1)–Ru(1)–C(1)	174.15(8)	174.02	100.64(14)	169.63(9)	171.15	174.90(3)
P(2)–Ru(1)–H(1)	85.20(8)	83.00	83.00(15)	87.90(8)	88.00	80.80(17)
N(3)/N(2)–Ru(1)–H(1)	173.60(8)	174.00	89.20(14)			170.60(17)
N(1)–Ru(1)–H(1)	86.30(8)	88.00	175.40(14)	80.70(8)	85.00	86.80(17)
C(1)–Ru(1)–H(1)	87.80(8)	86.00	83.60(14)	89.00(8)	86.00	88.10(18)
P(1)–Ru(1)–H(1)	85.60(8)	87.00	89.60(15)	89.10(8)	89.00	89.20(17)
C(1)–Ru(1)–Cl(1)				102.12(8)	100.08	
N(1)–Ru(1)–Cl(1)				88.17(5)	88.66	
P(1)–Ru(1)–Cl(1)				93.01(19)	92.92	
P(2)–Ru(1)–Cl(1)				90.34(19)	90.81	
H(1)–Ru(1)–Cl(1)				168.70(8)	174.00	
Ru(1)–C(1)–O(1)	176.90(2)	177.08	175.60(4)	174.50(2)	176.37	176.80(8)
Ru(1)–N(2)–C(52)				169.20(8)		169.20(8)
N–C–S			178.20(7)			177.30(12)

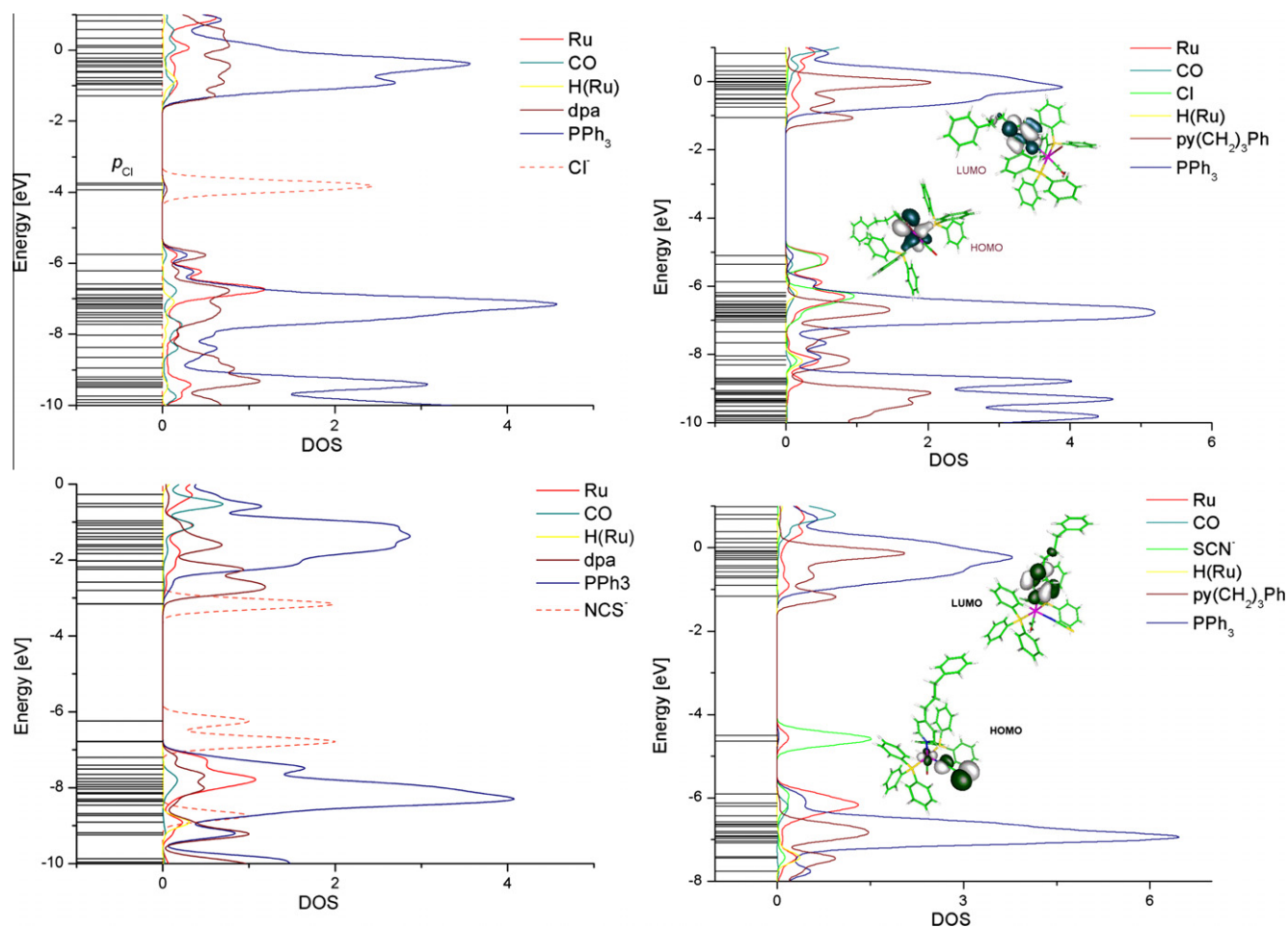


Fig. 3. The density of states (DOS) diagrams for the complexes.

Homo orbitals than the 4-(3-phenylpropyl)pyridine ligand. In the complexes, the LUMO orbitals are mainly localized on the pyridine derivative ligands. The d orbitals of the ruthenium central ions contribute in LUMO + 1 (neutral complexes **2** and **2a**) and LUMO + 3/+5 in the cationic complexes **1** and **1a**. Furthermore, the d_{Ru} orbitals are diffused in energy scope, corresponding to LUMO + 16 to LUMO + 20 levels. In these unoccupied orbitals, the carbonyl ligand plays a significant role. In Fig. 3, the dashed lines represent the orbitals of the chloride and thiocyanate anions in complexes **1** and **1a** respectively. It can be seen that thiocyanate is better matched in terms of energy to the molecular orbitals of the complex. In complexes **2** and **2a**, in which chloride and isothiocyanate ligands are in the coordination sphere, noticeable increases in the energy levels of HOMO orbitals with respect to the chloride complex occur. This change in energy levels of the molecular orbitals refers to the luminescent properties of the complexes.

The Mayer bond orders of the Ru–P, Ru–CO and Ru–H bonds are similar in the complexes and are close to 1.4, 2.6 and 1.7 respectively. The values of the bond orders between the ruthenium central ions and the N-donor ligands are also similar, and these are lower than 1 (close to 0.7), indicating the participation of ionic character in the bonds. The Ru–NCS bond order (0.9) is slightly lower than that of Ru–Cl (1.1) in complexes **2a** and **2** respectively. In order to compare the donor–acceptor properties of 2,2′-dipyridylamine and 4-(3-phenylpropyl)pyridine, NBO calculations were performed. The NBO analyses show that the donations from the ruthenium central ions to the pyridine derivative ligands have values 51.23 (53.26) and 24.23 (25.13) kcal/mol, and the back dona-

tions are 150.46 (163.45) and 52.97 (55.16) kcal/mol in the complexes **1** (**1a**) and **2** (**2a**) respectively. The data show the stronger donor–acceptor properties of 2,2′-dipyridylamine than 4-(3-phenylpropyl)pyridine.

3.2. Electronic spectra

The UV–Vis spectra of the studied chloride and thiocyanate complexes are similar and the maxima are located at 360.5, 310.4, 260.1, 213.3 and 327.0, 308.0, 255.5, 211.5 nm for complexes **1** and **1a** and 332.0, 256.2, 210.6 and 328.4, 276.2, 252.1, 211.0 nm for **2** and **2a** respectively. Assignments of the calculated transitions to the experimental bands are based on the criteria of energy and oscillator strength of the calculated transitions. In the description of the electronic transitions, only the main components of the molecular orbitals are taken into consideration. The electronic transitions were calculated with the application of the CAM-B3LYP functional, using the Coulomb-attenuating method.

The first transitions (above 300 nm) in the spectra have HOMO/HOMO – 1 → LUMO and HOMO → LUMO + 1/+3 character in the cationic and neutral complexes. The HOMO is localized on the d ruthenium orbitals with an admixture of π -PPh₃/dpa in **1**, **1a** and π -Cl/SCN in **2**, **2a** complexes. The LUMOs are localized on the pyridine derivatives and triphenylphosphine ligands, with a contribution of d_{Ru} , and Metal–Ligand Charge Transfer transitions are associated with these. The bands observed at 260, 255, 256 and 276 nm have been attributed to Metal–Ligand Charge Transfer transitions ($d \rightarrow \pi^*_{PPh_3/dpa/pyCHPh/Cl/SCN}$). In this energy region, the transitions

between the Homo \rightarrow LUMO + 8, Homo $- 7/-4/-3 \rightarrow$ LUMO + 2/+3 were calculated. The highest energy bands with maxima at 212 and 211 nm are attributed to transitions of Ligand–Ligand Charge Transfer type ($\pi \rightarrow \pi_{C=N}^*$).

The emission characteristics of the complexes have been examined in methanol solutions (with concentration of 5×10^{-4} mol/dm³) at room temperature. The excitations were executed at wavelengths corresponding to the maxima of the first electronic absorptions, *i.e.* at 360 nm for **1** and **1a**, and 330 nm for **2** and **2a**. The emission spectra are shown in Fig. 4. As can be seen in Fig. 4, the cationic complexes **1** and **1a** give stronger luminescence than the neutral complexes **2** and **2a**. It is associated with the participation of the pyridine derivative ligand orbitals in the frontier Homo orbitals of the complexes. The DOS diagrams show that 2,2'-dipyridylamine plays a role in the energy range adequate to frontier occupied orbitals, and in the case of the 4-(3-phenylpropyl)pyridine

ligand, its presence is only indicated for the lower Homo orbitals (Homo $- 4$ and below in energy). In the LUMO orbitals, the participation of the N-heteroaromatic ligands in all complexes is similar. Therefore an emission originating from the lowest energy metal to ligand charge transfer (MLCT) state, derived from the excitation involving a $d_{\pi} \rightarrow \pi_{\text{ligand}}$ transition, is observed. The assignment is also supported by the analysis of the frontier orbitals of the corresponding complexes showing a contribution of ligand nature. The complicated structure of the luminescence spectra suggests that more than one state is involved in the luminescence processes. Replacement of the chloride ligand with a thiocyanate ligand significantly increases the emission intensity, especially in the case of the cationic complex **1a**. In Fig. 3, the chloride and thiocyanate anions in complexes **1** and **1a** are presented by dashed lines. As one can see, the energies of the π -orbitals of the NCS⁻ ligands are well tuned to the levels of the molecular orbitals of the complex in contrast to

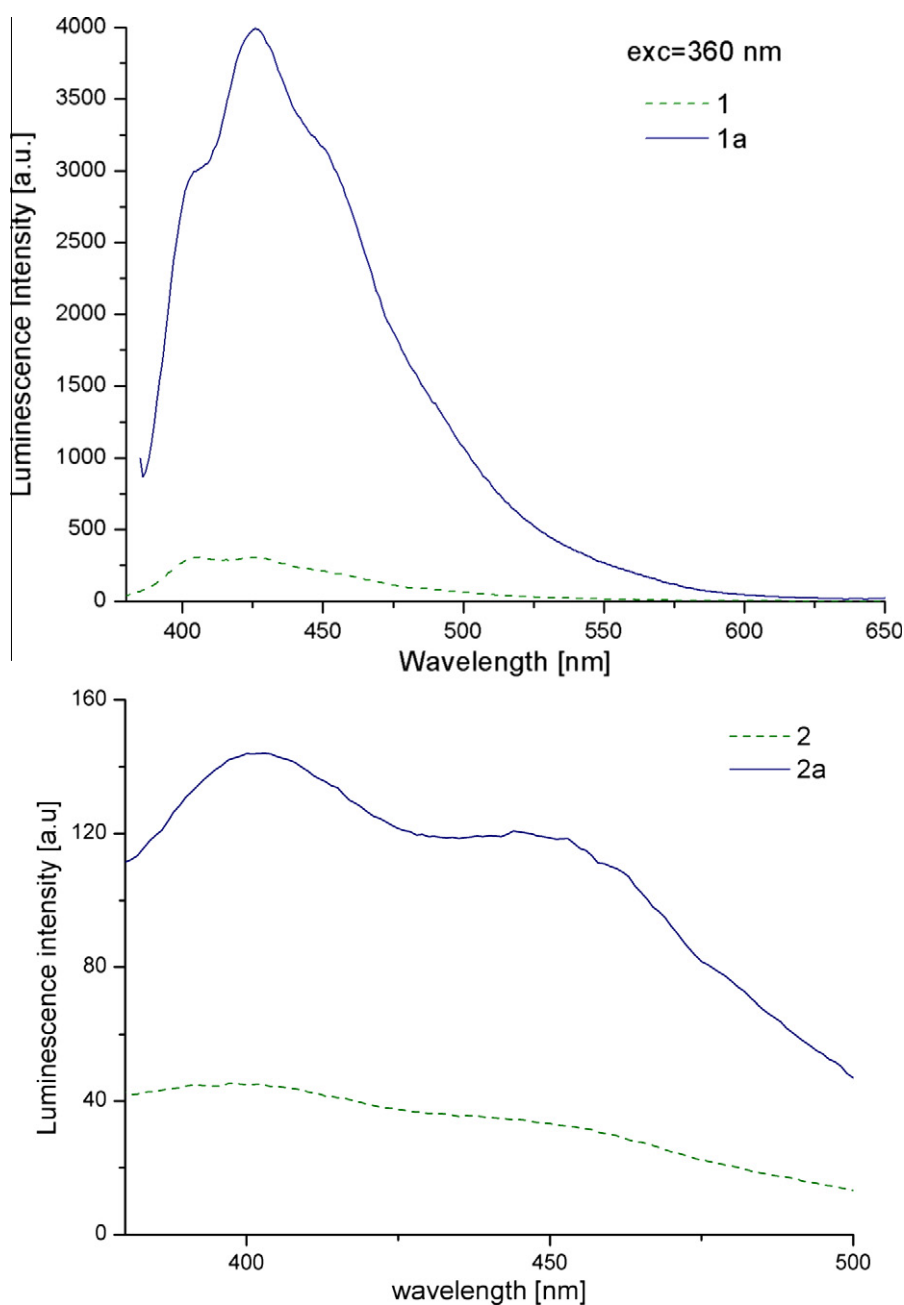


Fig. 4. The emissions spectra of the complexes **1**, **1a** and **2**, **2a** in methanolic solutions ($c = 5 \times 10^{-4}$ mol/dm³).

the energy of the *p* orbitals of Cl[−]. In the case of neutral complex **2a**, the isothiocyanate ligand shifts the Homo and Homo – 1 orbitals to a higher energy.

4. Conclusion

Summarizing, new ruthenium(II) complexes with pyridine derivative ligands have been synthesized. The molecular structures of the complexes were determined by X-ray crystallography, and the spectroscopic properties were studied using infrared, ¹H and ³¹P NMR spectra. Based on the crystal structures, computational studies were carried out in order to determine the electronic structures of the complexes. The results were used to compare the π-donor/acceptor properties of the pyridine type ligands. Electronic spectra were calculated with use of the TD-DFT method and the transitions characters were discussed in connection with structure of the molecular orbitals of the complexes. The emission properties of the complexes have been examined. Emissions originating from the lowest energy metal to ligand charge transfer (MLCT) state, derived from an excitation involving a d_π → π_{ligand} transition, are observed. The assignment is supported by the analysis of the frontier orbitals of the corresponding complexes showing a partial contribution of ligands nature. The thiocyanate derivative of the cationic complex with the 2,2'-dipyridylamine ligand exhibits a very intense luminescence compared to the chloride analog.

Appendix A. Supplementary data

CCDC 784657, 792144, 794419 and 798323 contain the supplementary crystallographic data for [RuH(CO)(dpa)(PPh₃)₂]Cl·dpa·CH₃OH, [RuH(CO)(dpa)(PPh₃)₂]SCN·H₂O·CH₃OH, [RuHCl(CO)(pyCHPh)(PPh₃)₂] and [RuH(SCN)(CO)(pyCHPh)(PPh₃)₂]. These data can be obtained free of charge via <http://www.ccdc.cam.ac.uk/conts/retrieving.html>, or from the Cambridge Crystallographic Data Centre, 12 Union Road, Cambridge CB2 1EZ, UK; fax: (+44) 1223-336-033; or e-mail: deposit@ccdc.cam.ac.uk. Calculations have been carried out in the Wrocław Centre for Networking and Supercomputing (<http://www.wcss.wroc.pl>)

References

- [1] M. Chandra, A.N. Sahay, D.S. Pandey, M.C. Puerta, P. Valerga, *J. Organomet. Chem.* 648 (2002) 39.
- [2] A.K. Singh, P. Kumar, M. Yadav, D.S. Pandey, *J. Organomet. Chem.* 695 (2010) 567.
- [3] B.J. Coe, S.J. Glenwright, *Coord. Chem. Rev.* 203 (2000) 5.
- [4] M.U. Raja, N. Gowri, R. Ramesh, *Polyhedron* 29 (2010) 1175.
- [5] R. Sivakumar, A.T.M. Marcelis, S. Anandan, *J. Photochem. Photobiol. A: Chem.* 208 (2009) 154.
- [6] T. Funaki, M. Yanagida, N. Onozawa-Komatsuzaki, Kaługa Kasuga, Y. Kawanishi, M. Kurashige, K. Sayama, H. Sugihara, *Inorg. Chem. Commun.* 12 (2009) 842.
- [7] N. Onozawa-Komatsuzaki, M. Yanagida, T. Funaki, K. Kasuga, K. Sayama, H. Sugihara, *Inorg. Chem. Commun.* 12 (2009) 1212.
- [8] S. Kannan, M. Sivagamasundari, R. Ramesh, Yu Liu, *J. Organomet. Chem.* 693 (2008) 2251.
- [9] M. Sivagamasundari, R. Ramesh, *Spectrochim. Acta, Part A* 67 (2007) 256.
- [10] M. Sivagamasundari, R. Ramesh, *Spectrochim. Acta, Part A* 66 (2007) 427.
- [11] M.V. Kaveri, R. Prabhakaran, R. Karvembu, K. Natarajan, *Spectrochim. Acta, Part A* 61 (2005) 2915.
- [12] M. Ulaganatha Raja, N. Gowri, R. Ramesh, *Polyhedron* 29 (2010) 1175.
- [13] E.M.J. Johansson, M. Odellius, M. Gorgoi, O. Karis, R. Ovsyannikov, F. Schäfers, S. Svensson, H. Siegbahn, H. Rensmo, *Chem. Phys. Lett.* 464 (2008) 192.
- [14] J.G. Małecki, *Polyhedron* 29 (2010) 1237.
- [15] J.G. Małecki, *Polyhedron* 29 (2010) 1973.
- [16] J.G. Małecki, *Polyhedron* 29 (2010) 2489.
- [17] J.G. Małecki, *Polyhedron* 29 (2011) 79.
- [18] N. Ahmad, J.J. Levinson, S.D. Robinson, M.F. Uttley, *Inorg. Synth.* 15 (1974) 48.
- [19] M.J. Frisch, G.W. Trucks, H.B. Schlegel, G.E. Scuseria, M.A. Robb, J.R. Cheeseman, G. Scalmani, V. Barone, B. Mennucci, G.A. Petersson, H. Nakatsuji, M. Caricato, X. Li, H.P. Hratchian, A.F. Izmaylov, J. Bloino, G. Zheng, J.L. Sonnenberg, M. Hada, M. Ehara, K. Toyota, R. Fukuda, J. Hasegawa, M. Ishida, T. Nakajima, Y. Honda, O. Kitao, H. Nakai, T. Vreven, J.A. Montgomery Jr., J.E. Peralta, F. Ogliaro, M. Bearpark, J.J. Heyd, E. Brothers, K.N. Kudin, V.N. Staroverov, R. Kobayashi, J. Normand, K. Raghavachari, A. Rendell, J.C. Burant, S.S. Iyengar, J. Tomasi, M. Cossi, N. Rega, J.M. Millam, M. Klene, J.E. Knox, J.B. Cross, V. Bakken, C. Adamo, J. Jaramillo, R. Gomperts, R.E. Stratmann, O. Yazyev, A.J. Austin, R. Cammi, C. Pomelli, J.W. Ochterski, R.L. Martin, K. Morokuma, V.G. Zakrzewski, G.A. Voth, P. Salvador, J.J. Dannenberg, S. Dapprich, A.D. Daniels, O. Farkas, J.B. Foresman, J.V. Ortiz, J. Cioslowski, D.J. Fox, *Gaussian 09, Revision A.1*, Gaussian Inc., Wallingford, CT, 2009.
- [20] A.D. Becke, *J. Chem. Phys.* 98 (1993) 5648; C. Lee, W. Yang, R.G. Parr, *Phys. Rev. B* 37 (1988) 785.
- [21] T. Yanai, D. Tew, N. Handy, *Chem. Phys. Lett.* 393 (2004) 51.
- [22] M.E. Casida, in: J.M. Seminario (Ed.), *Recent Developments and Applications of Modern Density Functional Theory, Theoretical and Computational Chemistry*, vol. 4, Elsevier, Amsterdam, 1996, p. 391.
- [23] K. Eichkorn, F. Weigend, O. Treutler, R. Ahlrichs, *Theor. Chim. Acc.* 97 (1997) 119.
- [24] E.D. Glendening, A.E. Reed, J.E. Carpenter, F. Weinhold, *NBO (version 3.1)*.
- [25] N.M. O'Boyle, A.L. Tenderholt, K.M. Langner, *J. Comp. Chem.* 29 (2008) 839.
- [26] Adam L. Tenderholt, *QMForge, Version 2.1*, Stanford University, Stanford, CA, USA.
- [27] O.V. Dolomanov, L.J. Bourhis, R.J. Gildea, J.A.K. Howard, H. Puschmann, *J. Appl. Crystallogr.* 42 (2009) 339.
- [28] G.M. Sheldrick, *Acta Crystallogr., Sect. A* 64 (2008) 112.